International Journal of Nanomedicine

Dovepress
open access to scientific and medical research

Open Access Full Text Article

ORIGINAL RESEARCH

Combined Silver Sulfadiazine Nanosuspension with Thermosensitive Hydrogel: An Effective Antibacterial Treatment for Wound Healing in an Animal Model

Xiaoya Liu[1,2], Haiyang Fan[3], Zhiyun Meng[2], Zhuona Wu[2], Ruolan Gu[2], Xiaoxia Zhu[2], Hui Gan[2], Guifang Dou[2]

[1]Department of Pharmacy, Shenzhen Children's Hospital, Shenzhen, Guangdong Province, 518026, People's Republic of China; [2]Department of Pharmaceutical Sciences, Beijing Institute of Radiation Medicine, Academy of Military Medical Sciences, Beijing, 100850, People's Republic of China; [3]Department of Thoracic Surgery, The Seventh Affiliated Hospital, Sun Yat-sen University, Shenzhen, Guangdong Province, 518102, People's Republic of China

Correspondence: Guifang Dou; Hui Gan, Department of Pharmaceutical Sciences, Beijing Institute of Radiation Medicine, Academy of Military Medical Sciences, Beijing, 100850, People's Republic of China, Tel +86 10 66932951, Fax +86 10 66931993, Email dougf@bmi.ac.cn; ganh2003@163.com

Introduction: Silver sulfadiazine (AgSD) is widely used in burn wound treatment due to its broad-spectrum antibacterial activity. However, its application in wound healing is greatly hindered by the low solubility of AgSD particles and their cellular cytotoxicity. Herein, we studied the safety and in vivo efficacy of nano-sized silver sulfadiazine loaded in poloxamer thermosensitive hydrogel (NS/Gel).

Methods: In NS/Gel, silver sulfadiazine was prepared into silver sulfadiazine nanosuspension (NS) to improve the solubility and enhance its antibacterial activity, whereas the poloxamer thermosensitive hydrogel was selected as a drug carrier of NS to achieve slow drug release and reduced cytotoxicity. The acute toxicity of silver sulfadiazine nanosuspension was first evaluated in healthy mice, and its median lethal dose (LD_{50}) was calculated by the modified Karber method. Furthermore, in vivo antibacterial effect and wound healing property of NS/Gel were evaluated on the infected deep second-degree burn wound mice model.

Results: The mortality ratio of mice was concentration-dependent, and the LD_{50} for silver sulfadiazine nanosuspension was estimated to be 252.1 mg/kg (230.8 to 275.4 mg/kg, 95% confidence limit). The in vivo dosages used for burn wound treatment (40–50 mg/kg) were far below LD_{50} (252.1 mg/kg). NS/Gel significantly accelerated wound healing in the deep second wound infection mice model, achieving > 85% wound contraction on day 14. *Staphylococcus aureus* in the wound region was eradicated after 7 days in NS/Gel group, while the bacterial colony count was still measurable in the control group. Histological analysis and cytokines measurement confirmed that the mice treated with NS/Gel exhibited well-organized epithelium and multiple keratinized cell layers compared to control groups with the modulated expression of IL-6, VEGF, and TGF-β.

Conclusion: The combination of silver sulfadiazine nanosuspension and thermo-responsive hydrogel has great potential in clinical burn wound treatment.

Keywords: silver sulfadiazine, antibacterial agent, thermosensitive hydrogel, acute toxicity, burn wound model, median lethal dose

Introduction

Burn wounds pose a serious public health problem worldwide. In 2018, World Health Organization (WHO) reported that some 180,000 deaths were caused by burn wounds.[1] Managing the severity of burn wound injury and associated inflammation are significant clinical challenges.[2–4] The healing process and severity of burn wounds are affected by several factors, such as the degree of burn, the microbial burden, chronic diseases etc.[5,6] For patients with > 40% of total body surface area being burned, approximately 75% die of infection-related complications. Therefore, an effective antibacterial agent that could prevent severe infection and accelerate wound healing is urgently needed.

The topical application of antibacterial agents has been widely accepted as an effective way to alleviate cutaneous infections.[7–10] Among them, silver sulfadiazine (AgSD) is considered the "gold standard" in treating burn wound

Received: 16 November 2022
Accepted: 1 February 2023
Published: 11 February 2023

infections.[11,12] AgSD has dual-action on bacterial growth.[12] The sulfa moiety can prevent bacterial folate absorption and DNA synthesis, while the silver ions released from AgSD can bind and disrupt the DNA structure and replication. Besides, AgSD eradicates biofilms by killing bacteria through the co-work of sulfadiazine and silver ions.[14] However, the antibacterial activity of AgSD is commonly discounted because of its poor aqueous solubility (slightly soluble, 7.8 mg/mL) and cellular cytotoxicity.[15–17] Therefore, frequent applications of commercial AgSD cream are required to achieve the therapeutic drug concentration at the administration site. Furthermore, secondary injury inevitably occurs during a dressing change due to the external force applied on the wound to remove residual cream before applying new cream.[12,18] To overcome these problems, an effective method that could improve the aqueous solubility of AgSD is urgently needed.

Nanotechnology is widely used for improving drug solubility, which is achieved by significantly enlarging the surface area and the surface-volume ratio of drug particles.[19,20] Therefore, we employed a high-pressure homogenization method to prepare the AgSD coarse powders into nano-size.[21] In vitro analysis demonstrated that AgSD nanosuspension (NS) could dissolve within 3 minutes, which was significantly improved compared with coarse powder. Besides, the poloxamer-based thermosensitive hydrogel was selected as the drug carrier for topical silver sulfadiazine nanosuspensions delivery to form the silver sulfadiazine nanosuspension loaded thermos-responsive hydrogel (NS/Gel). Furthermore, the in-situ phase transition property of the poloxamer-based hydrogel makes it a perfect choice for thorough coverage of wounds regardless of their shape, size, and depth.[22]

Since the toxicity of silver sulfadiazine is commonly ascribed to the accumulation of silver ions, it remained unclear whether the increased solubility would aggravate the toxicity.[23] To the best of our knowledge, no previous study evaluated the toxicity of AgSD nanosuspension. Besides, the in vivo therapeutical evaluation is of essential importance to demonstrate the efficacy of NS/Gel.

In this work, we investigated the acute toxicity of NS by calculating the LD_{50} and evaluating the accumulation of silver ions in main organs. Moreover, a reliable and reproducible deep second-degree burn wound model was used to test the antibacterial activity and wound healing properties of NS/Gel. Finally, we compared the wound healing progress of mice treated with NS/Gel, commercial AgSD cream, and other formulations in macroscopic and microscopic views. Overall, the present study aimed to comprehensively investigate the safety and effectivity of NS/Gel and provide preclinical profiles for further research.

Materials and Methods

The Preparation and Characterization of Silver Sulfadiazine Nanosuspensions-Loaded Hydrogel

Silver sulfadiazine nanosuspensions were prepared by the high-pressure homogenization method. 1.5% poloxamer 407 (w/v%) solution was prepared as a dispersion solution, after which 20 g of silver sulfadiazine coarse powder was added to 180 mL of the previously prepared 1.5% P407 solution. To obtain a uniform system, we first pre-milled the mixture with Ultra Turrax (T25, IKA, Germany) at 10,000 rpm for 10 min. Next, uniform suspensions were circulated at 200, 400, 600, and 800 bars for 2 cycles, followed by 20 cycles at 1200 and 1400 bars using AH100D high-pressure homogenizer (ATS Engineering Inc., Shanghai, China). Finally, the silver sulfadiazine nanosuspension was stored at 4°C and protected from light. Gels were prepared on a weight/weight basis using the cold method. Briefly, poloxamer 407 (P407), poloxamer 188 (P188), and glycerol (Gly) were accurately weighed to obtain a suspension with 18% P407, 2% P188, and 10% glycerol. The solutions were preserved at 4°C for ≥ 24 h to ensure complete dissolution. Finally, 10 mL of silver sulfadiazine nanosuspension (100 mg/mL) was slowly added to 90 mL of hydrogel and then stirred for 10 min to obtain AgSD/NS-loaded hydrogel (NS/Gel). The drug was accurately measured using UHPLC to ensure the homogeneity of the mixture.

The surfaces of hydrogels within or without AgSD were measured using a scanning electron microscope (Hitachi SU8010; Hitachi Ltd., Tokyo, Japan). In addition, the phase transition temperature ($T_{sol-gel}$) of NS/Gel was measured using a Brookfield digital viscometer (model DV-III; Brookfield Engineering Laboratories, Inc., USA).

Acute Toxicity Measurement

The acute toxicity of NS was investigated to evaluate its safety. The modulated Karber method was designed to obtain the median lethal dose (LD_{50}).

Kunming mice (20–25 g) were purchased from Beijing Vital River Laboratory Animal Technology Co., Ltd, Beijing, PR China. The protocol in this study was reviewed and approved by the ethical committee of the Academy of Military Medical Sciences. (Approval ID: IACUC-DWZX-2021-735). The model fully conformed to the requirements in the Ministry of Science and Technology Guide for the Care and Use of Laboratory Animals (GB/T 35892-2018). At first, the animals were acclimatized at a temperature of 25 ± 2°C and relative humidity of 70 ± 5% under natural light/dark conditions for one week. They had access to food and water ad libitum. Before burn wound creation, anesthesia was performed with pentobarbital sodium (45 mg/kg, Biomedical, Beijing).

A total of 50 mice were randomly divided into five groups, each one including 5 male and 5 female mice. The mice fasted for 24h before treatment. The dosage ratio was set as 0.668, and the dosages were 100, 150, 224, 335, 501, and 750 mg/kg. After intraperitoneal administration, mice fasted for the first 4 hours while they had free access to drinking water. Changes in hair, physical condition, skin, and death were continuously observed and recorded during seven days of treatment. Their body weight was recorded on days 0, 1, 3, 5, and 7. The day of administration was considered day 0. The LD_{50} was calculated with its 95% confidence limit using modulated Karber method. Besides, the total number of dead mice was recorded for each group. After 7 days, mice were sacrificed, and residual silver ions in organs, including the brain, heart, spleen, liver, lung, and kidneys, were measured by inductively coupled plasma mass spectrometry (ICP-MS).[24]

In vivo Wound Healing Studies

The Induction of Deep Second-Degree Burn Mice Model

Staphylococcus aureus (ATCC 25923), a gram-positive bacterium, was the bacterial strain used in the present study. The strain was cultivated at 37°C in Luria Bertani (LB) or Luria Bertani agar medium. First, an isolated colony was picked and inoculated in normal saline to prepare bacterial suspensions of 0.5 McFarland standard. Then, the bacterial suspensions with a concentration of 10^8 colony-forming units (CFU) /mL were obtained.

The mice deep second-degree burn wound model was developed following the approach previously described by Guo et al.[25] Briefly, the mice were intraperitoneally anesthetized by pentobarbital (45 mg/kg), after which the surface of their dorsal area was shaved with electoral clippers, and the residual hair was removed by commercial depilatory cream (VEET™; Reckitt Benckiser, NSW, Australia). A precision temperature-controlled scald apparatus was used to create burn injuries to the dorsum (Figure 1A and C). The $3^{\#}$ thermal contact head with a diameter of 1.5 cm was selected to produce a deep second-degree burn wound. The thermal contact head was heated to 80°C and then pressed against the bare dorsum skin for 8 seconds. The pressure exerted on the skin was 500 g. In order to create an infectious wound, 100 μL of the prepared bacterial suspensions were subcutaneously injected in mice 15 minutes after burn induction (Figure 1A).

All these animals were randomly divided into five experimental groups. Each group has 20 mice. The specific treatment for each group is listed in Table 1. Regardless of the treatment agent, the injection volume was 100 μL. The uninfected group was subcutaneously injected with 100 μL of physiological saline instead of the bacterial suspension. Twenty-four hours after injury, the animals received the first treatment stipulated for each experimental group. The wound site was treated every two days for 7 days (Figure 1B).

Measurement of Wound Healing Rate

In order to compare the wound healing properties of different formulations, a digital camera (Canon PowerShot G7 X Mark ii/iii) was used to record progressive changes in the wound area. To precisely calculate the wound area, a ruler was placed on the side of the wound. Image J software was applied to quantify the wound area. The wound areas were digitally photographed on 0, 1, 3, 5, 7, and 14 days post-wounding. The following equation was used to measure the wound contraction rate:

$$Wound\ contraction\ rate\ \% = [(Initial\ wound\ area - Specific\ day\ wound\ area)/Initial\ wound\ area]^{*}100$$

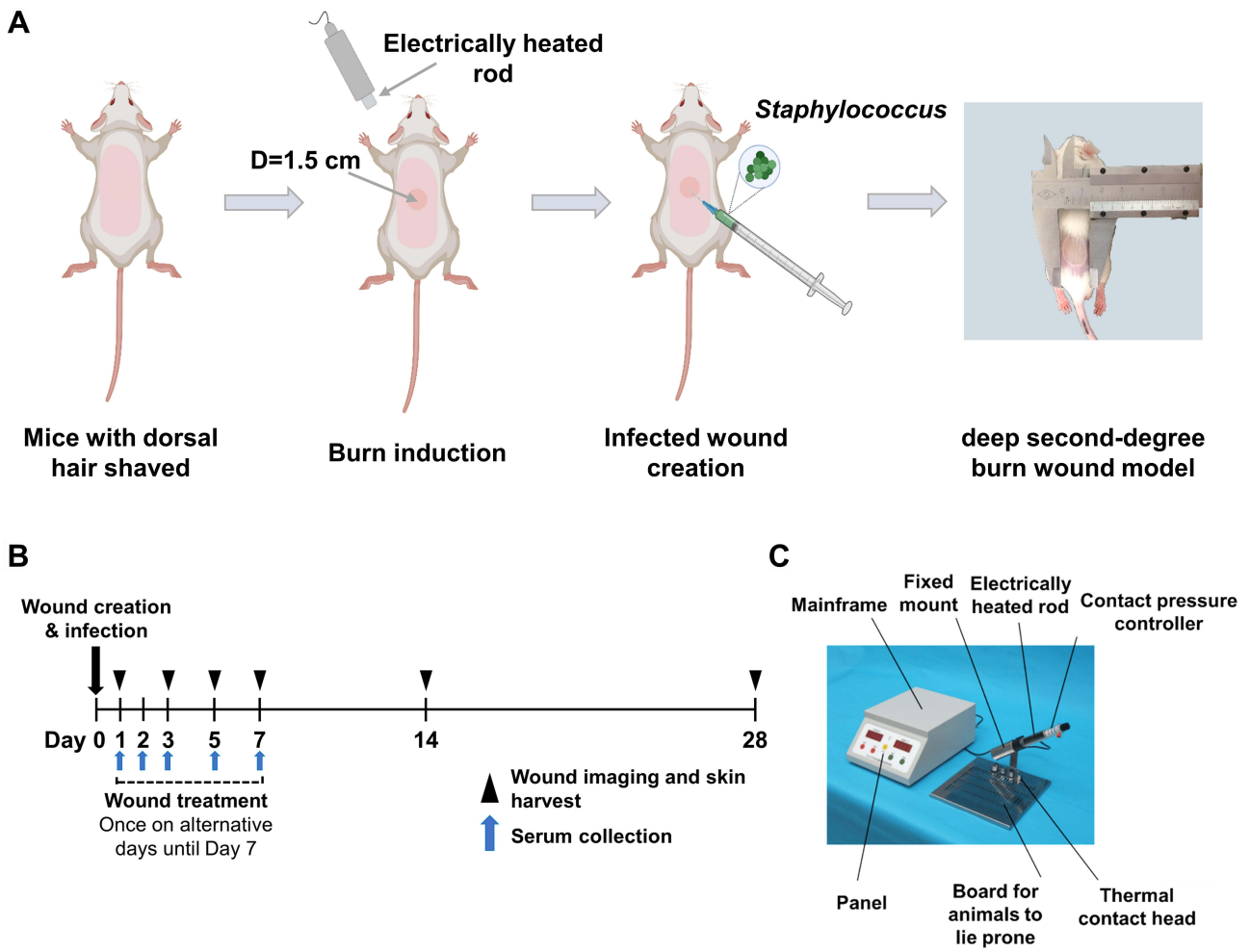

Figure 1 Burn wound induction and treatment. (**A**) Flow chart of burn wound creation. (**B**) Schematic illustration of burn wound treatments. (**C**) Diagram of the precision temperature-controlled scald apparatus.

Moreover, the time needed for the scab to fall off from burned mice was also considered as one of the parameters for assessing the wound healing process. Scab-off time is defined as the time the scar fell off the wound sites.

Quantification of Bacteria in Wound Sites

The antibacterial activities of different formulations were evaluated by measuring the local bacterial load reduction. The mice were killed at 1, 2, 3, 5, and 7 days after the first treatment, and a circular piece of wound skin was immediately excised from each mouse with an 8-mm diameter sterile biopsy punch. The tissue specimens were weighted and homogenized with 1 mL sterile physiological saline by a tissue grinder. Then, the mixture was consecutively diluted in sterile physiological saline. Finally, 0.1 mL of each bacterial dilution was plated onto LB agar in an incubator at 37°C.

Table 1 The Specific Treatment of Each Group

Group	Burn	Bacterial	Treatment
Uninfected (Blank)	√	–	0.9% NaCl
Control (Ctrl)	√	√	0.9% NaCl
Gel	√	√	Blank gel
NS/Gel	√	√	AgSD/NS gel
Cream	√	√	AgSD Cream

Abbreviation: AgSD, silver sulfadiazine.

After 24 h, the number of bacterial colonies was counted and multiplied by the corresponding dilution factor and reported as a colony-forming unit (CFU) per gram of tissues.

Histopathological Analysis

The skin sections were acquired on day 28 and evaluated by light microscopy examination to assess morphological alterations during the wound healing process. Hematoxylin and eosin stains were applied to determine the inflammation reaction, while the Masson stain mainly focused on collagen distribution. Specifically, skin pieces from the wound area were collected and fixed in 4% paraformaldehyde (PFA). Dehydration was achieved by a series of ethanol solutions and finally embedded in paraffin wax. Thin paraffin sections (5 μm) were prepared and stained with Harris's hematoxylin and eosin and Masson's trichrome staining dyes.

Quantification of Cytokines by Enzyme-Linked Immunosorbent Assay

Serums were collected at 12h, and 1, 3, 5, and 7 days post-treatment, and the levels of vascular endothelial growth factor A (VEGF-A), interleukin 6 (IL-6), and transforming growth factor β (TGF-β) were measured with commercial cytokine-specific ELISA kits (R&D systems, USA).

Data Analysis

Data were expressed as the mean ± standard deviation (SD). Datasets were tested for a normal distribution using the Shapiro–Wilk's test, and differences between the group means were estimated by using a one-way analysis of variance (ANOVA) with Tukey's test. A P value < 0.05 (95%) was considered statistically significant.

Results and Discussion

In vitro Evaluation of Silver Sulfadiazine Nanosuspension and Silver Sulfadiazine Nanosuspension Loaded Hydrogel

As illustrated in Figure 2A, AgSD coarse powder was milled and homogenized into nanoparticles. The average particle size of AgSD nanosuspension was approximately 291.7 nm, with a polydispersity index (PDI) of 0.288. The particle size of AgSD nanosuspension was stable during storage at 4°C for 6 months.[21] Poloxamer hydrogel was chosen due to its high biocompatibility and thermosensitive properties.[12,22] We speculated that the AgSD/NS was packaged into hydrogel during the gelation process (Figure 2A). Specifically, the individual block copolymers (unimer) can self-assemble into micelles at a concentration higher than the critical micellar concentration and temperature higher than gelation temperature (32°C was set in the present work, Figure 2B). Likewise, by further increasing the temperature, the micelles could form 3D networks (hydrogels) with higher viscosity.[26] Skin temperature was influenced by ambient temperature and personal physiology conditions like neurophysiology, disease, gender, and age.[13,27] The mean skin temperature of an average individual exposed to a neutral environment has been reported to range from 30 to 34°C, while people with regional infection usually have higher skin temperature.[13,28] The gelation temperature we used was around 32°C, which is the temperature at which the viscosity experienced abrupt change. A typical viscosity change against the temperature curve is shown in Figure 2C. A significant change in viscosity was observed from 2750 ± 375 cP at 30°C to 37,187.5 ± 437.5 cP at 35°C. This indicated that the poloxamer matrix was quickly transferred from solution to semi-solid gel when the temperature was beyond the specific gelation temperature. The proposed drug loading mechanism was identified in SEM images. The microstructure of NS/Gel was rougher and more irregular compared to the control gel, which indicated that AgSD/NS might embed in the micelles' core when phase transition occurred (Figure 2D). As shown in Figure 2E, the thickness of NS/Gel was approximately 493.7±38.2 nm while the thickness of Gel was about 186.3±12.6 nm. Since the diameter of AgSD nanosuspensions was approximately 290 nm, which was in accordance with the difference value of thickness between Gel and NS/Gel, we deduced that the AgSD was evenly embedded in the gel wall when phase transition happened.

Two typical parameters, inhibition zone and minimal inhibition concentration (MIC), were selected to evaluate the antimicrobial potency of AgSD coarse powder (Bulk), AgSD nanosuspension (NS), and AgSD nanosuspension loaded hydrogel (NS/Gel) (Figure 2F and G). As expected, NS exhibited a higher antibacterial effect against *P. aeruginosa* and

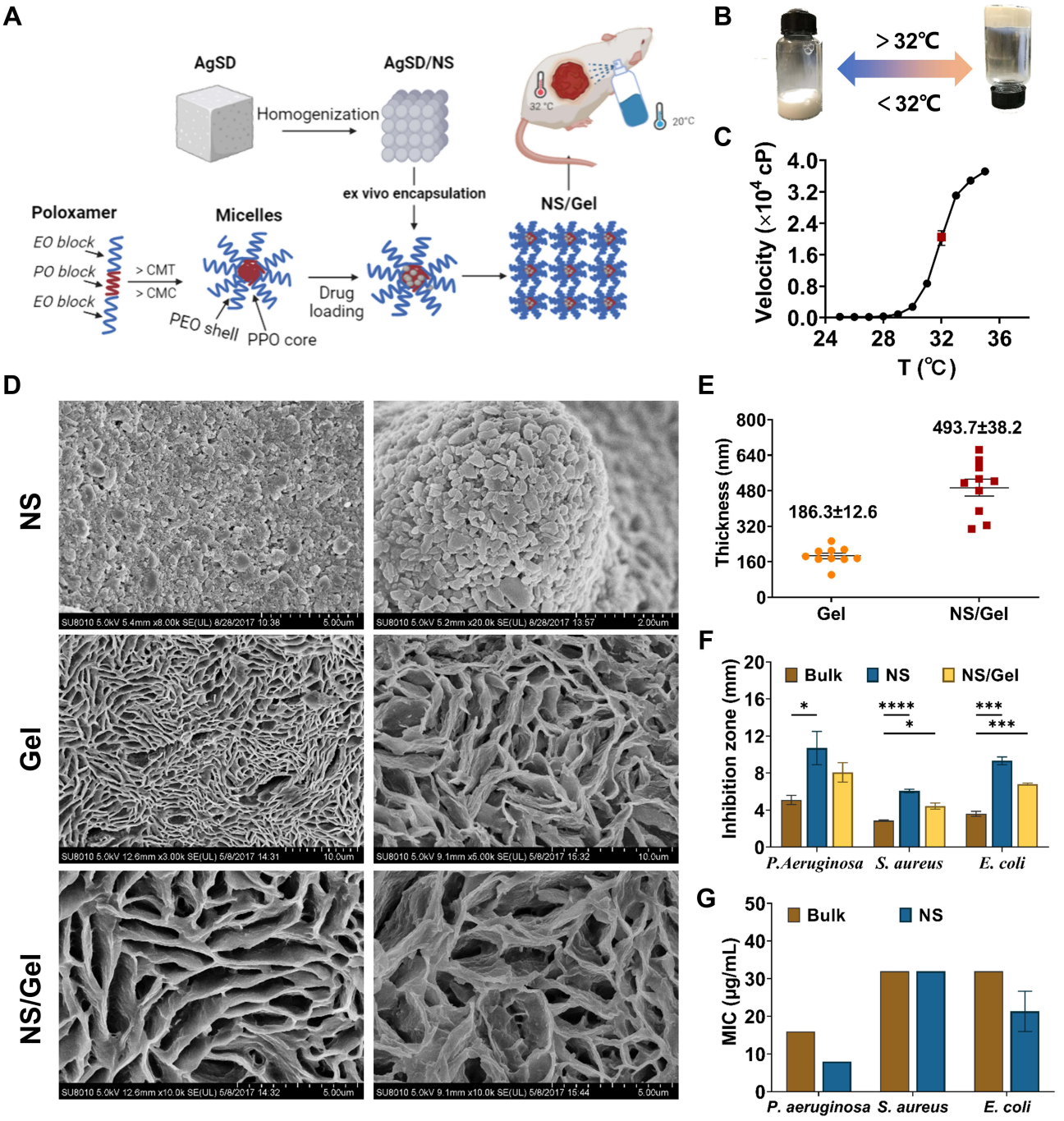

Figure 2 Preparation and characterization of NS/Gel. (**A**) Schematic diagram of generation of silver sulfadiazine nanosuspension loaded thermosensitive hydrogel system. (**B**) Images of NS/Gel in relation to changes in temperature. NS/Gel was gelled when the temperature went up to 32°C. (**C**) Viscosity change of NS/Gel with temperature. The red square indicates the gelation temperature of NS/Gel. (**D**) Microscopy images of silver sulfadiazine nanosuspension (NS), blank gel (Gel), and silver sulfadiazine loaded hydrogel (NS/Gel). (**E**) The network wall thickness of Gel and NS/Gel. (**F** and **G**) In vitro antibacterial activity. Inhibition zone (**F**) and MIC (**G**) were selected as critical parameters to compare the therapeutic effect. P value: *<0.05; ***<0.001, ****<0.0001.

Abbreviations: NS, silver sulfadiazine nanosuspension; NS/Gel, silver sulfadiazine nanosuspension loaded thermosensitive hydrogel; Bulk, AgSD coarse powder; MIC, minimum inhibition concentration.

E. coli, Gram-negative bacteria, than against Gram-positive *S. aureus*. According to previous studies, AgSD has an excellent potential effect against Gram-negative bacteria compared to Gram-positive.[29] The MIC value of NS against *P. aeruginosa* was 8 μg/mL, which revealed half reduced MIC compared with Bulk (16 μg/mL) (Figure 2G). Similarly, the inhibition zone of NS was significantly higher than Bulk against all three strains. Despite a slight decrease in the

inhibition zone compared with NS, the antibacterial effect of NS/Gel was considerably higher than Bulk against *S. aureus* and *E. coli* (Figure 2F). Overall, the in vitro evaluation of effectiveness proved that NS/Gel was an ideal and potential therapeutic agent for the healing of infected wounds.

Acute Toxicity Assessment

Few studies investigated the acute toxicity of AgSD since topical administration of AgSD has been reported to be safe with less systematic toxicity.[15] Common side effects of AgSD, such as argyria, renal toxicity, and transient leucopenia, were found to be proportional to silver concentration.[30,31] To the best of our knowledge, no previous study investigated the toxicity of silver sulfadiazine on the nanoscale. Considering the possible toxicity caused by a significant change in diameter, we investigated the acute toxicity of NS in the present study.

According to the China Food and Drug Administration, an administration method that enables drug exposure to the system is mandatory. Thus, the intraperitoneal injection was used to achieve systematic exposure to NS. The median lethal dose (LD_{50}) was calculated by the modulated Karber method while the silver ions accumulation in tissues was measured by the previously built ICP-MS method.[24]

Reduced activity and weakness were observed in mice treated with high dosages (>335 mg/kg). The group treated with a concentration of 750 mg/kg had an enlarged liver. No visible alterations were witnessed in the organs of other groups. The mortality ratio of mice was concentration-dependent (Table 2), and LD_{50} for NS was estimated to be 252.1 mg/kg (230.8 to 275.4 mg/kg, 95% confidence limit) (Figure 3A). The dosage we used in following wound treatment (approximately 40–50 mg/kg) was far from LD_{50}.

The content of silver ions in six organs was measured. The residual silver ions in tissues were concentration-dependent. The liver had the highest level of silver ions, followed by the spleen, kidney, lung, heart, and brain (Figure 3B). These results were consistent with the distribution of silver nanoparticles in organs, including the liver, spleen, lung, kidney, and brain.[32,33] No silver was measured in mice organs treated with NS < 150 mg/kg. The obtained results indicated that the dosage we used was safe. In their study, Wasef LG measured the deposition of silver after daily administration of AgSD in burn wound mice model over 28 days of treatment, finding that the liver was the most critical organ for silver kinetics, which was consistent with our research.[34] Limited data are available on the residual silver ions in organs after silver sulfadiazine administration. Despite no visible abnormalities in organs, further studies are needed to evaluate the long-term toxicity of silver sulfadiazine nanosuspensions to provide more information for clinical use.

In vivo Wound Healing Efficacy of Silver Sulfadiazine Nanosuspension Loaded Thermosensitive Hydrogel

In the present study, we created a uniform and reproducible deep second-degree burn wound model with precision temperature-control apparatus (Figure 2C). The burn temperature on the mice's dorsum, the burn time, and the pressure exerted on the mice's skin were all controllable by this apparatus.[35] A 100 μL bacterial suspension was injected into the burn site to obtain an infected wound, thus inducing an ideal deep second burn wound combined infection mice model. Commercial silver sulfadiazine cream was used as a positive control to demonstrate the enhanced antibacterial activity of

Table 2 Mortality Ratio of Silver Sulfadiazine Nanosuspensions. (n=10)

Group	n	Dosage (mg/kg)	Mortality (%)
1	10	100	0
2	10	150	20
3	10	224	40
4	10	335	70
5	10	501	90
6	10	750	100

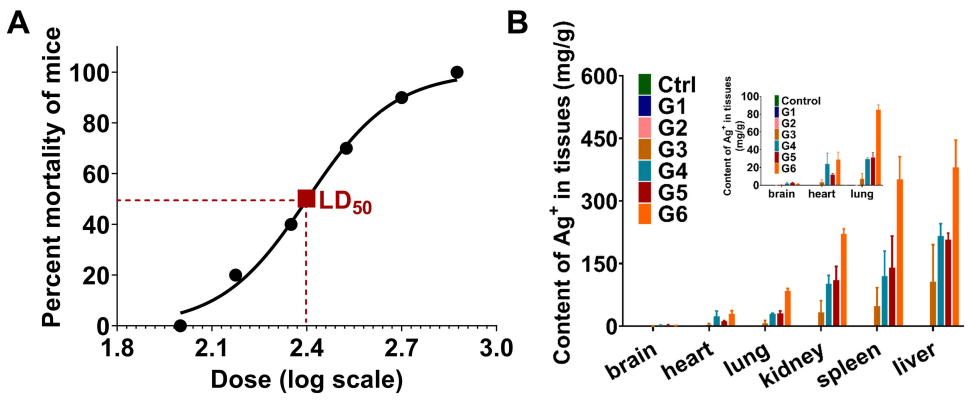

Figure 3 Acute toxicity of silver sulfadiazine nanosuspension. (**A**) Dosage response mortality curves of silver sulfadiazine nanosuspension. (**B**) Cumulative content of silver ions in organs.

the prepared NS/Gel. The NS/Gel was found to have enhanced antimicrobial activity against *Staphylococcus aureus* and accelerated wound healing properties.

Wound Contraction Rate Analysis

Representative images of deep second-degree burn wounds in mice are illustrated in Figure 4A. Healing happens instantly after wound creation, followed by edema and tissue fluid secreting. The wound areas became enlarged in the Ctrl group and Gel group on day 3, while groups treated with antibacterial agents gradually contracted towards the wound center. The death rates of mice from the five groups are recorded in Figure 4B. As indicated in Figure 4B, 30% percent of mice in the Control group died on day 5, while only 20% percent died in the Gel group. Since the application of poloxamer on deep second-degree burn wounds at the early stage was reported to alleviate wound deepening, we speculated that the hydrogel alone also contributed to wound healing.[3] Lower death rates were measured in the Cream and NS/Gel groups compared to the Control group, indicating that the application of an antibacterial agent might influence the death rate in the early stage. The wound contraction rates of different groups are illustrated in Figure 4D, and all groups were compared with NS/Gel on other days. The contraction rate of NS/Gel was significantly higher than Ctrl, especially in the early stage (<7 days). This might be due to the antibacterial activity of NS, which has an important role in wound healing by inhibiting bacterial growth.[34] After seven days, the NS/Gel was the only formulation that achieved > 85% wound contraction rate in mice and was significantly better than commercial cream on day 14 (87%±6% vs 74%±8%) ($P<0.01$). The average weight of all groups slightly decreased on day 3 because of the inflammation reaction following continuous increase until day 28 (Figure 4C). No significant difference was found among all groups.

As shown in Figure 4A, scars in NS/Gel and Cream group formed on day 3, which was earlier than in other groups. On day 7, scars began to slough. The time needed for scars to fall off from the burned wound is shown in Figure 4E. There was no significant difference in the time needed for the scab to fall off between the NS/Gel and Cream group. The slightly shorter scab-off time in the Cream group might be due to the silver sulfadiazine and the formulation additives.[17] As expected, an accelerated wound-healing process was observed in mice from the Gel group. Poloxamer was reported to be able to early alleviate wound deepening, indicating that blank gel can be used as a potential wound dressing for uninfected wound sites.[22,36] Overall, the wound healing property of NS/Gel was much better than that of commercial AgSD cream.

Bacterial Growth Inhibition

As burn wounds are susceptible to infections, it is of vital importance to eradicate the bacteria from the infectious sites for rapid wound healing.[3] *Staphylococcus aureus* is one of the most common bacterial strains affecting the skin of burn patients.[37] The bacteria in the wound areas were collected and counted at different time intervals after treatment, according to the approach previously reported by Saymen et al.[38] The CFUs were calculated on days 1, 2, 3, 5, and 7. The Blank group was used to exclude the possible environmental contamination during the experiment. The change in bacterial burden reduction in the wound area is summarized in Figure 5A.

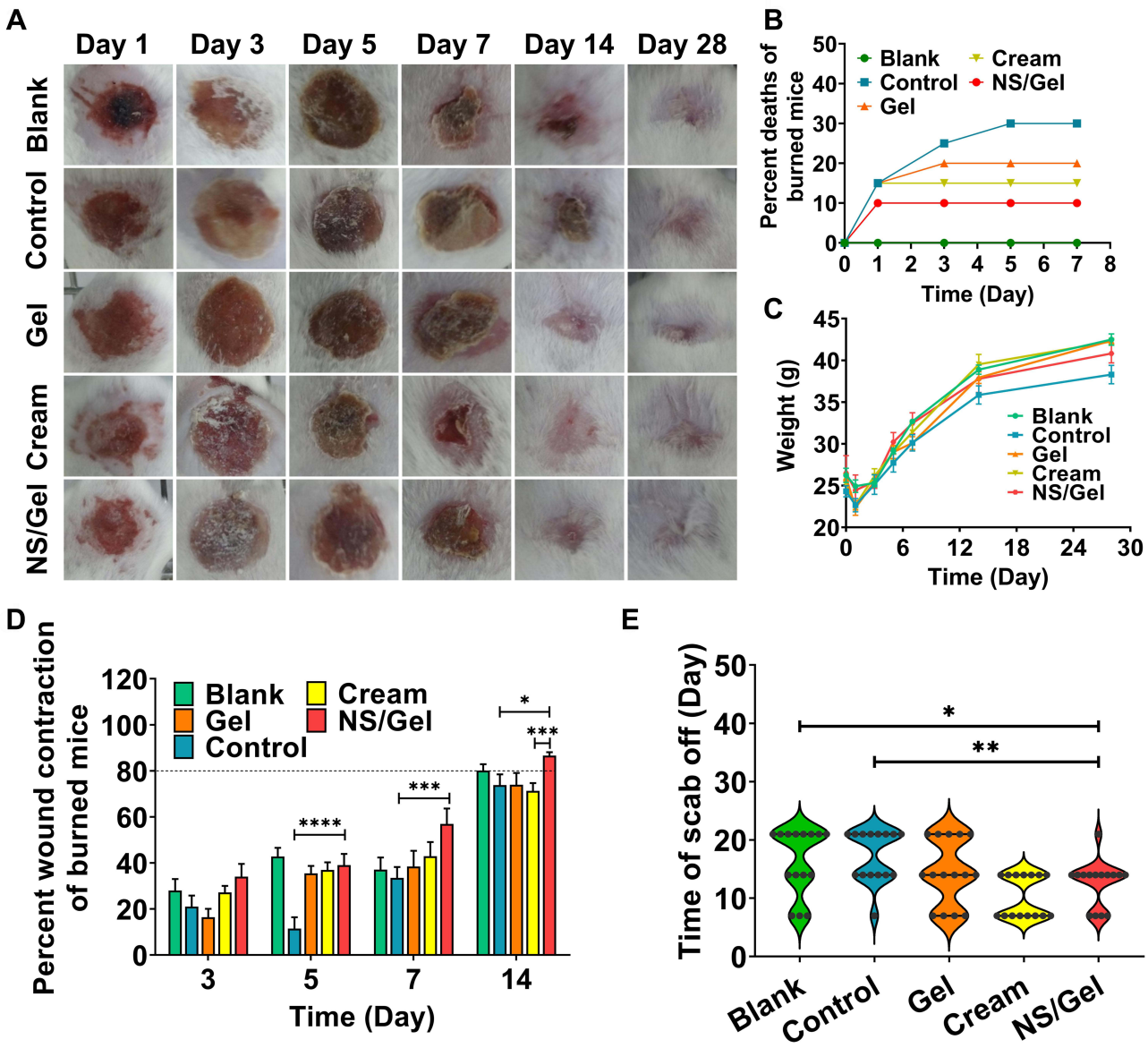

Figure 4 Evaluation of wound healing process in deep second burn wound. (**A**) Macroscopic images of wound area in mice treated by five different formulations. (**B**) The percent deaths of burned mice in five groups. (**C**) The average weight of each group was plotted against time. (**D**) Percent wound contraction of burned mice. The dotted line represents the 80% wound healing rate. (**E**) The scabby-off time was recorded. P value: P value: *<0.05; **<0.01; ***<0.001, ****<0.0001.
Abbreviations: NS, silver sulfadiazine nanosuspension; NS/Gel, silver sulfadiazine nanosuspension loaded thermosensitive hydrogel.

Mice treated with formulations containing antibacterial agents showed lower bacterial counts compared to the control group. The bacterial colony count in the Cream group revealed a slight increase on day 2, decreasing furthermore to 3.8×10^8 CFU/g on day 7. Conversely, bacterial growth in NS/Gel group steadily decreased during 7 days from 9.8×10^8 to 0 CFU/g. Taking advantage of the higher solubility and nano-size scale, bacterial count in NS/Gel mice group significantly decreased compared to the Cream group on days 2, 3, and 7. As illustrated in Figure 5B, the residual silver ion in the blood of NS/Gel was higher than Cream in the first 7 days, which is reasonable because of the higher solubility of NS. The silver subsequently decreased to < 200 ng/mL and was similar to the residual silver of AgSD cream. NS/Gel eradicated *S. aureus* infection at day 7, demonstrating its ability to reduce infection after prolonged treatment.

Histopathology Analysis

On day 28, the skin in the wound site was collected from the surviving animals for light microscopic examination. The samples were longitudinally cross-sectioned and stained with hematoxylin and eosin (H&E) and Masson trichrome (Figure 6).

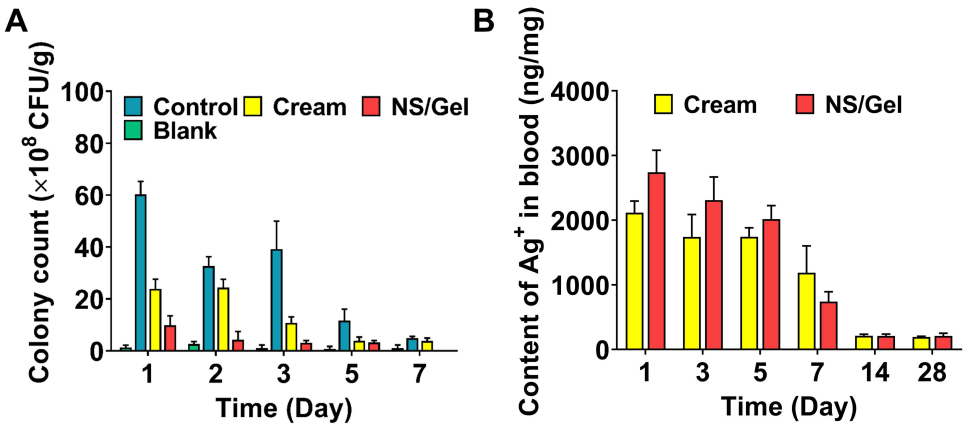

Figure 5 (**A**) Bacterial colony count in wound area was measured for Blank, Control, Cream, and NS/Gel groups. (**B**) Content of silver ions in mice blood treated by Cream and NS/Gel group on different days.
Abbreviations: NS, silver sulfadiazine nanosuspension; NS/Gel, silver sulfadiazine nanosuspension loaded thermosensitive hydrogel.

The new epidermis was found in all groups, especially in the NS/Gel group. A well-organized epithelium and multiple keratinized cell layers, like those found in normal skin, were observed in the NS/Gel group, while in the Control group, many neutrophils (blue arrow) remained at wound sites with fewer typical skin structures (Figure 6A). Besides, the epidermis was well differentiated in NS/Gel group, as was confirmed by more hair follicles (yellow triangle) and sweat glands (blue triangle). Few skin appendages were observed in the Cream group.

Furthermore, the neat arrangement of collagen fibers (yellow arrow) could be seen in the NS/Gel group dermis, which was cluttered or missing in other groups. Although mice treated with AgSD cream had the shortest scab-off time, they showed thin epidermal layers with immature collagen fibers arranged in parallel on day 28 (Figure 6A). Surprisingly, the Gel group demonstrated more accelerated wound healing compared to the control group, which is consistent with previous research.[39,40] The collagen volume fraction (CVF) was also calculated according to the Masson staining images by Image J software. The results are illustrated in Figure 6B. The application of wound dressings accelerated collagen formation. No significant difference was observed between Cream and NS/Gel. Overall, skin samples from the NS/Gel-treated group showed a well-organized epidermis, complete restoration of epidermal layers, and basal, granular, and cornfield layers.

Quantification of Cytokines

Severe wound burn often cause the dysregulation of various cytokines, which has a critical role in multiple stages of the wound healing process, including inflammation reaction, reconstruction of blood vessels, and fibroblast proliferation.[41] IL-6, VEGF-A, and TGF-β1 are mainly evolved in three stages of wound healing: the inflammatory stage, granulation tissue formation, and production of collagen fiber.[42] As a result, IL-6, VEGF-A, and TGF-β1 were selected to compare the healing process after different treatments.

The effects of different treatments on IL-6 expression levels are illustrated in Figure 6C. All groups experienced increased expressions of IL-6 on the first day, which then decreased in the following days. The increased IL-6 expression of all groups indicated the inflammation reaction after wound induction, which was consistent with the advance in the wound healing process.[3] The concentration of IL-6 treated by NS/Gel on day 1 was 182.4 pg/mL, which was far less than the Control group (279.6 pg/mL). Meanwhile, the group treated with Cream was 219 pg/mL. At 3 days post cutaneous injury, the Control group still had high serum levels of IL-6, a cytokine released by inflammatory cells in excessive inflammation.

Considering its vital role in vasculogenesis, which can support metabolic activity for cell proliferation and collagen synthesis, we used VEGF-A.[43,44] The average serum concentrations of VEGF are illustrated in Figure 6D. The concentration of VEGF treated by NS/Gel was 155.3 pg/mL on day 3, which was significantly different from all other

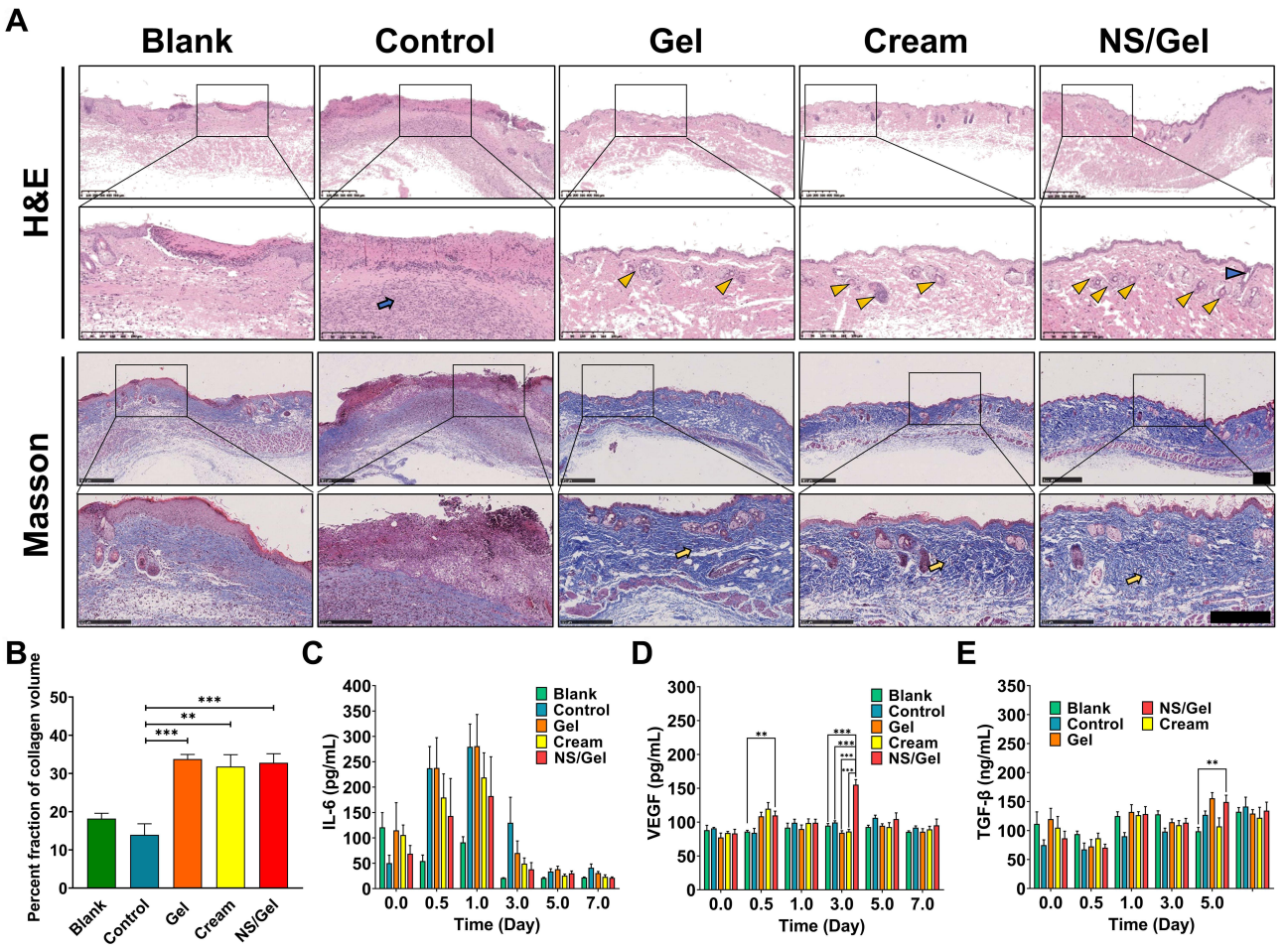

Figure 6 Histopathology analysis. (**A**) Hematoxylin and eosin (H&E) staining and Masson trichrome dye staining of mice dorsum biopsies. Cross-sections through the longitudinal aspect of the scarred areas were made. Magnification: upper: 10x; down: 15x. Blue arrow: neutrophil; yellow triangle: hair follicle; blue triangle: sweat gland; yellow arrow: collagen fiber. (**B**–**D**) Expression of cytokines in mice serum. (**E**) The percent fraction of collagen volume fraction (CFV) was calculated using Masson images. Scale bars: 250 μm. P value: **<0.01; ***<0.001.

Abbreviations: NS, silver sulfadiazine nanosuspension; NS/Gel, silver sulfadiazine nanosuspension loaded thermosensitive hydrogel.

groups ($p < 0.5$). The elevated expression of VEGF in the NS/Gel group might be ascribed to the AgSD nanoparticles and poloxamer hydrogel.

TGF-β1 can increase the expression of type I collagen and has a determining effect on wound healing and fibrosis.[5,45] The serum concentration of TGF-β1 is shown in Figure 6E. The secretion of TGF-β1 fluctuated for 7 days for all groups. The expression of TGF-β1 in the NS/Gel group increased from 113.5 ng/mL on Day 3 to 149.3 ng/mL on Day 5. Interestingly, the gel group also showed high expression of TGF-β1 on day 1 (132.1 ng/mL) and day 5 (155.6 ng/mL), which could be due to the healing promotion activity of poloxamer.[36] Since TGF-β1 can simulate the fibroblast to produce dense collagen networks, the increased expression of TGF-β1 in the Gel group and NS/Gel group might contribute to the wound healing process on day 5. Correspondingly, the wound contraction rates of the Gel group and NS/Gel group also slightly increased from day 3 to day 5. (Figure 4D) Afterwards, the TGF-β levels in the infected wounds decreased to the same level as Blank. No visible scar formation was observed in NS/Gel group according to Figure 4A, which indicated that the increased expression of TGF-β1 in the early stage did not induce fibrosis in the wound site.

Conclusion

The present study thoroughly evaluated the effectiveness and safety of silver sulfadiazine nanosuspension-loaded thermosensitive hydrogel. In vitro characterization demonstrated that the NS/Gel was feasible upon critical gelling

temperature. Meanwhile, compared with coarse powder, enhanced antibacterial activity was measured *against P. aeruginosa, E. coli*, and *S. aureus*. A designed acute toxicity test calculated the LD_{50} value of silver sulfadiazine nanosuspension for the first time, confirming the safety of the dosage used in wound healing.

A reproducible and reliable infectious deep second wound mice model was built to compare the i*n vivo* activity of NS/Gel with other formulations in this work. A combination of silver sulfadiazine nanosuspension and thermosensitive hydrogel exhibited an accelerated wound healing process more effectively than commercial silver sulfadiazine cream while significantly decreasing the bacterial burden in mice. Overall, NS/Gel resulted as a promising antibacterial formulation for the treatment of infected burn wounds.

Acknowledgments

This work has been funded by the Beijing Municipal Natural Science Foundation (NO.7202148). The authors wish to thank Dr. Zheng for their technical assistance in the measurement of gelation temperature.

Disclosure

The authors report no conflicts of interest in this work.

References

1. World Health Organazation. Burns. Fact Sheets. 2018. Available from: https://www.who.int/news-room/fact-sheets/detail/burns. Accessed February 2, 2023.
2. Gurtner GC, Werner S, Barrandon Y, Longaker MT. Wound repair and regeneration. *Nature*. 2008;453(7193):314–321. doi:10.1038/nature07039
3. Liu YF, Ni PW, Huang Y, Xie T. Therapeutic strategies for chronic wound infection. *Chin J Traumatol*. 2022;25(1):11–16. doi:10.1016/j.cjtee.2021.07.004
4. Jeschke MG, van Baar ME, Choudhry MA, Chung KK, Gibran NS, Logsetty S. Burn injury. *Nat Rev Dis Primers*. 2020;6(1):11. doi:10.1038/s41572-020-0145-5
5. Khan I, Rahman SU, Tang E, et al. Accelerated burn wound healing with photobiomodulation therapy involves activation of endogenous latent TGF-beta1. *Sci Rep*. 2021;11(1):13371. doi:10.1038/s41598-021-92650-w
6. Roy DC, Tomblyn S, Isaac KM, et al. Ciprofloxacin-loaded keratin hydrogels reduce infection and support healing in a porcine partial-thickness thermal burn. *Wound Repair Regen*. 2016;24(4):657–668. doi:10.1111/wrr.12449
7. Norbury W, Herndon DN, Tanksley J, Jeschke MG, Finnerty CC. Infection in burns. *Surg Infect*. 2016;17(2):250–255. doi:10.1089/sur.2013.134
8. Krausz AE, Adler BL, Cabral V, et al. Curcumin-encapsulated nanoparticles as innovative antimicrobial and wound healing agent. *Nanomedicine*. 2015;11(1):195–206. doi:10.1016/j.nano.2014.09.004
9. Wu P, Chen D, Yang H, et al. Antibacterial peptide-modified collagen nanosheet for infected wound repair. *Smart Mater Bull*. 2021;2:172–181. doi:10.1016/j.smaim.2021.06.002
10. Yin W, Wang Q, Zhang J, et al. A dynamic nano-coordination protein hydrogel for photothermal treatment and repair of infected skin injury. *J Mater Chem B*. 2022;10(40):8181–8185. doi:10.1039/d2tb01146h
11. Alkhatib D, Zelai N. Preparation, characterization and stability of silver sulfadiazine nanoliposomes. *Trop J Pharm Res*. 2022;20(4):665–671. doi:10.4314/tjpr.v20i4.1
12. Joshi N, Mishra N, Rai VK. Development and evaluation of in situ gel of silver sulfadiazine for improved therapeutic efficacy against infectious burn wound. *J Pharm Innov*. 2021;16(3):537–550. doi:10.1007/s12247-020-09464-y
13. Park TH, Park S, Yu S, et al. Highly sensitive on-skin temperature sensors based on biocompatible hydrogels with thermoresponsive transparency and resistivity. *Adv Healthc Mater*. 2021;10(14):e2100469. doi:10.1002/adhm.202100469
14. Ueda Y, Miyazaki M, Mashima K, et al. The effects of silver sulfadiazine on methicillin-resistant Staphylococcus aureus biofilms. *Microorganisms*. 2020;8(10):1551. doi:10.3390/microorganisms8101551
15. Hollinger MA. Toxicological aspects of topical silver pharmaceuticals. *Crit Rev Toxicol*. 1996;26(3):255–260. doi:10.3109/10408449609012524
16. Handayani E, Masithoh RF. A small-scale re-evaluation of the efficacy of silver sulfadiazine for burns. *Br J Community Nurs*. 2020;25(Sup12):S34–S38. doi:10.12968/bjcn.2020.25.Sup12.S34
17. Gao L, Gan H, Meng Z, et al. Evaluation of genipin-crosslinked chitosan hydrogels as a potential carrier for silver sulfadiazine nanocrystals. *Colloids Surf B Biointerfaces*. 2016;148:343–353. doi:10.1016/j.colsurfb.2016.06.016
18. Yabanoglu H, Basaran O, Aydogan C, Azap OK, Karakayali F, Moray G. Assessment of the effectiveness of silver-coated dressing, chlorhexidine acetate (0.5%), citric acid (3%), and silver sulfadiazine (1%) for topical antibacterial effects against the multi-drug resistant Pseudomonas aeruginosa infecting full-skin thickness burn wounds on rats. *Int Surg*. 2013;98(4):416–423. doi:10.9738/INTSURG-D-13-00017.1
19. Kesharwani SS, Bhat GJ. Formulation and nanotechnology-based approaches for solubility and bioavailability enhancement of zerumbone. *Medicina*. 2020;56(11):557. doi:10.3390/medicina56110557
20. Zhang X, Li Z, Gao J, et al. Preparation of nanocrystals for insoluble drugs by top-down nanotechnology with improved solubility and bioavailability. *Molecules*. 2020;25(5). doi:10.3390/molecules25051080
21. Liu X, Gan H, Hu C, et al. Silver sulfadiazine nanosuspension-loaded thermosensitive hydrogel as a topical antibacterial agent. *Int J Nanomedicine*. 2019;14:289–300. doi:10.2147/IJN.S187918

22. Alvarado-Gomez E, Martinez-Castanon G, Sanchez-Sanchez R, Ganem-Rondero A, Yacaman MJ, Martinez-Gutierrez F. Evaluation of anti-biofilm and cytotoxic effect of a gel formulation with Pluronic F-127 and silver nanoparticles as a potential treatment for skin wounds. *Mater Sci Eng C Mater Biol Appl*. 2018;92:621–630. doi:10.1016/j.msec.2018.07.023
23. Mimura ECM, Favoreto JPM, Favero ME, et al. Silver serum levels in burned patients treated with silver sulfadiazine and its toxicity on inflammatory cells. *Burns*. 2020;46(5):1120–1127. doi:10.1016/j.burns.2019.11.012
24. Shi Q, Ju M, Zhu X, et al. Pharmacokinetic properties of arsenic species after intravenous and intragastrical administration of arsenic trioxide solution in cynomolgus macaques using HPLC-ICP-MS. *Molecules*. 2019;24(2):241–258. doi:10.3390/molecules24020241
25. Guo Y, Baumgart S, Stark HJ, Harms H, Muller S. Mass cytometry for detection of silver at the bacterial single cell level. *Front Microbiol*. 2017;8:1326. doi:10.3389/fmicb.2017.01326
26. Filingeri D. Neurophysiology of skin thermal sensations. *Compr Physiol*. 2016;6(3):1429. doi:10.1002/cphy.c150040
27. Saxena A, Saha V, Ng EYK. Skin temperature maps as a measure of carotid artery stenosis. *Comput Biol Med*. 2020;116:103548. doi:10.1016/j.compbiomed.2019.103548
28. van Netten JJ, Prijs M, van Baal JG, Liu C, van der Heijden F, Bus SA. Diagnostic values for skin temperature assessment to detect diabetes-related foot complications. *Diabetes Technol Ther*. 2014;16(11):714–721. doi:10.1089/dia.2014.0052
29. Ahmadian S, Ghorbani M, Mahmoodzadeh F. Silver sulfadiazine-loaded electrospun ethyl cellulose/polylactic acid/collagen nanofibrous mats with antibacterial properties for wound healing. *Int J Biol Macromol*. 2020;162:1555–1565. doi:10.1016/j.ijbiomac.2020.08.059
30. Fuller FW. The side effects of silver sulfadiazine. *J Burn Care Res*. 2009;30(3):464–470. doi:10.1097/BCR.0b013e3181a28c9b
31. Wan AT, Conyers RA, Coombs CJ, Masterton JP. Determination of silver in blood, urine, and tissues of volunteers and burn patients. *Clin Chem*. 1991;37(10 Pt 1):1683–1687. doi:10.1093/clinchem/37.10.1683
32. Lankveld DP, Oomen AG, Krystek P, et al. The kinetics of the tissue distribution of silver nanoparticles of different sizes. *Biomaterials*. 2010;31(32):8350–8361. doi:10.1016/j.biomaterials.2010.07.045
33. Recordati C, De Maglie M, Bianchessi S, et al. Tissue distribution and acute toxicity of silver after single intravenous administration in mice: nano-specific and size-dependent effects. *Part Fibre Toxicol*. 2016;13:12. doi:10.1186/s12989-016-0124-x
34. Wasef LG, Shaheen HM, El-Sayed YS, et al. Effects of silver nanoparticles on burn wound healing in a mouse model. *Biol Trace Elem Res*. 2020;193(2):456–465. doi:10.1007/s12011-019-01729-z
35. Oh KT, Bronich TK, Kabanov AV. Micellar formulations for drug delivery based on mixtures of hydrophobic and hydrophilic pluronic block copolymers. *J Control Release*. 2004;94(2–3):411–422. doi:10.1016/j.jconrel.2003.10.018
36. Baskaran H, Toner M, Yarmush ML, Berthiaume F. Poloxamer-188 improves capillary blood flow and tissue viability in a cutaneous burn wound. *J Surg Res*. 2001;101(1):56–61. doi:10.1006/jsre.2001.6262
37. Haidari H, Bright R, Strudwick XL, et al. Multifunctional ultrasmall AgNP hydrogel accelerates healing of S. aureus infected wounds. *Acta Biomater*. 2021;128:420–434. doi:10.1016/j.actbio.2021.04.007
38. Saymen DG, Nathan P, Holder IA, Hill EO, Macmillan BG. Infected surface wound: an experimental model and a method for the quantitation of bacteria in infected tissues. *Appl Microbiol*. 1972;23(3):509–514. doi:10.1128/am.23.3.509-514.1972
39. Yuhua S, Ligen L, Jiake C, Tongzhu S. Effect of poloxamer 188 on deepening of deep second-degree burn wounds in the early stage. *Burns*. 2012;38(1):95–101. doi:10.1016/j.burns.2010.06.002
40. Bae IH, Park JW, Kim DY. Enhanced regenerative healing efficacy of a highly skin-permeable growth factor nanocomplex in a full-thickness excisional mouse wound model. *Int J Nanomedicine*. 2014;9:4551–4567. doi:10.2147/IJN.S68399
41. Kubo H, Hayashi T, Ago K, Ago M, Kanekura T, Ogata M. Temporal expression of wound healing-related genes in skin burn injury. *Leg Med*. 2014;16(1):8–13. doi:10.1016/j.legalmed.2013.10.002
42. Wang LL, Zhao R, Liu CS, et al. A fundamental study on the dynamics of multiple biomarkers in mouse excisional wounds for wound age estimation. *J Forensic Leg Med*. 2016;39:138–146. doi:10.1016/j.jflm.2016.01.027
43. Ruan Q, Zhao C, Ye Z, Ruan J, Xie Q, Xie W. Effect and possible mechanism of monocyte-derived VEGF on monocyte-endothelial cellular adhesion after electrical burns. *Burns*. 2015;41(4):825–832. doi:10.1016/j.burns.2014.10.030
44. Kim JW, Jeong H, Yang MS, Lim CW, Kim B. Therapeutic effects of zerumbone in an alkali-burned corneal wound healing model. *Int Immunopharmacol*. 2017;48:126–134. doi:10.1016/j.intimp.2017.05.005
45. Li CW, Wang Q, Li J, et al. Silver nanoparticles/chitosan oligosaccharide/poly(vinyl alcohol) nanofiber promotes wound healing by activating TGFbeta1/Smad signaling pathway. *Int J Nanomedicine*. 2016;11:373–386. doi:10.2147/IJN.S91975